



Static and Dynamic Strength of Scarf-Repaired Thick-Section Composite Plates

**by Bazle A. Gama, Stephane Mahdi, Curt Cichanowski,
Shridhar Yarlagadda, and John W. Gillespie, Jr.**

ARL-CR-549

September 2004

prepared by

**Center for Composite Materials
University of Delaware
Newark, DE 19716**

under contract

DAAD19-01-2-0005

NOTICES

Disclaimers

The findings in this report are not to be construed as an official Department of the Army position unless so designated by other authorized documents.

Citation of manufacturer's or trade names does not constitute an official endorsement or approval of the use thereof.

Destroy this report when it is no longer needed. Do not return it to the originator.

Army Research Laboratory

Aberdeen Proving Ground, MD 21005-5069

ARL-CR-549

September 2004

Static and Dynamic Strength of Scarf-Repaired Thick-Section Composite Plates

**Bazle A. Gama, Stephane Mahdi, Curt Cichanowski,
Shridhar Yarlagadda, and John W. Gillespie, Jr.
Center for Composite Materials
University of Delaware, Newark, DE**

prepared by

**Center for Composite Materials
University of Delaware
Newark, DE 19716**

under contract

DAAD19-01-2-0005

REPORT DOCUMENTATION PAGE			<i>Form Approved</i> OMB No. 0704-0188		
Public reporting burden for this collection of information is estimated to average 1 hour per response, including the time for reviewing instructions, searching existing data sources, gathering and maintaining the data needed, and completing and reviewing the collection information. Send comments regarding this burden estimate or any other aspect of this collection of information, including suggestions for reducing the burden, to Department of Defense, Washington Headquarters Services, Directorate for Information Operations and Reports (0704-0188), 1215 Jefferson Davis Highway, Suite 1204, Arlington, VA 22202-4302. Respondents should be aware that notwithstanding any other provision of law, no person shall be subject to any penalty for failing to comply with a collection of information if it does not display a currently valid OMB control number. PLEASE DO NOT RETURN YOUR FORM TO THE ABOVE ADDRESS.					
1. REPORT DATE (DD-MM-YYYY) September 2004		2. REPORT TYPE Final		3. DATES COVERED (From - To) November 2002–March 2003	
4. TITLE AND SUBTITLE Static and Dynamic Strength of Scarf-Repaired Thick-Section Composite Plates			5a. CONTRACT NUMBER DAAD19-01-2-0005 (CMT)		
			5b. GRANT NUMBER		
			5c. PROGRAM ELEMENT NUMBER		
6. AUTHOR(S) Bazle A. Gama, Stephane Mahdi, Curt Cichanowski, Shridhar Yarlagadda, and John W. Gillespie, Jr.			5d. PROJECT NUMBER 622618.AH80		
			5e. TASK NUMBER		
			5f. WORK UNIT NUMBER		
7. PERFORMING ORGANIZATION NAME(S) AND ADDRESS(ES) Center for Composite Materials University of Delaware Newark, DE 17916			8. PERFORMING ORGANIZATION REPORT NUMBER		
9. SPONSORING/MONITORING AGENCY NAME(S) AND ADDRESS(ES) U.S. Army Research Laboratory ATTN: AMSRD-ARL-WM-MB Aberdeen Proving Ground, MD 21005-5069			10. SPONSOR/MONITOR'S ACRONYM(S) ARL-CR-549		
			11. SPONSOR/MONITOR'S REPORT NUMBER(S)		
12. DISTRIBUTION/AVAILABILITY STATEMENT Approved for public release; distribution is unlimited.					
13. SUPPLEMENTARY NOTES					
14. ABSTRACT Composite structural armor is typically a sandwich construction consisting of thick-section composite, rubber, and ceramic layers, which are combined to provide an optimal balance of structural and ballistic performance at minimum weight. Our focus was on the scarf repair of the thick-section plain weave S-2 Glass/SC15 composite subjected to static and dynamic loading. Deliberate damage to backing plates was repaired at elevated temperatures using induction heating and at room temperature. The static response of control and repaired plates was compared via four-point bend testing. The effect of three scarf angles and four repair adhesives was quantified. Using these repair techniques, renewal of stiffness was achievable, except for the case of the highly ductile, low-stiffness adhesive. The renewal of moment capacity of the repair beams was highly dependent on the scarf angle for various adhesives, and a maximum renewal of strength was 60%. The dynamic strength of scarf patch-repaired composite specimens was investigated through axial compression strength testing using a split-Hopkinson bar. Under dynamic loading, the axial strength was found to be dependent on the scarf angle and rate of loading. Loci of failure are reported for the various materials, scarf angles, and loading conditions.					
15. SUBJECT TERMS repair, induction cure, thick-section composites, axial compression, Hopkinson bar, failure analysis, punch shear test, energy absorption, S-2 Glass/SC15, hybrid					
16. SECURITY CLASSIFICATION OF:			17. LIMITATION OF ABSTRACT UL	18. NUMBER OF PAGES 38	19a. NAME OF RESPONSIBLE PERSON Bazle A. Gama
a. REPORT UNCLASSIFIED	b. ABSTRACT UNCLASSIFIED	c. THIS PAGE UNCLASSIFIED			19b. TELEPHONE NUMBER (Include area code) 302-831-8352

Contents

List of Figures	iv
List of Tables	iv
Acknowledgments	v
1. Introduction	1
2. Test Methods	3
3. Materials and Repair Procedure	4
3.1 Materials	4
3.2 Repair Procedure	5
4. Induction Repair	5
5. Static Performance of Scarf-Repaired Composite Beams	7
6. Dynamic Axial Compression of Scarf-Repaired Composite Plates	9
7. Conclusions	12
8. References	14
Distribution List	16

List of Figures

Figure 1. Cross section of a model four-layer structural armor (5).	1
Figure 2. Ballistic damage of a composite structural armor: (a) the ceramic tiles after the cover layer have been removed and (b) cross section (8).....	2
Figure 3. Four-point bending testing of scarf-repaired composite backing plate.	3
Figure 4. Hopkinson bar procedure for dynamic axial compression of scarf repair composite specimens.	4
Figure 5. Induction-heating of the elevated-temperature cure adhesives.	6
Figure 6. The renewal in static strength of the repaired backing plates.	8
Figure 7. Hopkinson bar responses of Hysol EA9359.3 induction-cured scarf-repaired composite specimens under axial compression.	10
Figure 8. Stress equilibrium in Hysol EA9359.3 scarf-repaired composite specimens.....	10
Figure 9. Stress analysis of scarf-repaired composite specimens under dynamic axial compressive load.....	11
Figure 10. Axial compressive strength of scarf-repaired composite specimens under dynamic compressive load.....	11
Figure 11. Fracture surfaces of scarf-repaired composite specimens under dynamic axial compression.	11
Figure 12. Stresses at failure in the rotated coordinate system of the scarf-repaired composite specimens.....	12

List of Tables

Table 1. Bending stiffness (per unit width) of the repaired backing plates.	7
Table 2. Bending moment at failure of the repaired baking plates.....	8

Acknowledgments

The authors wish to acknowledge the financial support provided by the Strategic Environmental Research and Development Program (grant no. DAAL01-98-K-0058) and the Composite Materials Technology Collaborative Program sponsored by the U.S. Army Research Laboratory under Cooperative Agreement DAAD19-01-2-0005.

INTENTIONALLY LEFT BLANK.

1. Introduction

Composite structural armor typically consists of different material layers stacked together to provide unique structural and ballistic properties, as well as satisfying other multifunctional requirements (e.g., fire, smoke, and toxicity [FST] resistance, electromagnetic shielding, etc.) (1–4). This program used a simplified four-layer configuration that consists of a composite cover layer for durability, a layer of ceramic tile for ballistic protection, a rubber layer, and a thick composite backing plate for structural and ballistic performance (figure 1). Fabrication of the composites used the vacuum assisted resin transfer molding (VARTM) process, which has been shown to provide superior mechanical properties in a single-step operation as compared to bonding individual layers in a multistep process (5). Additional details on structural behavior can be found in (5–7).

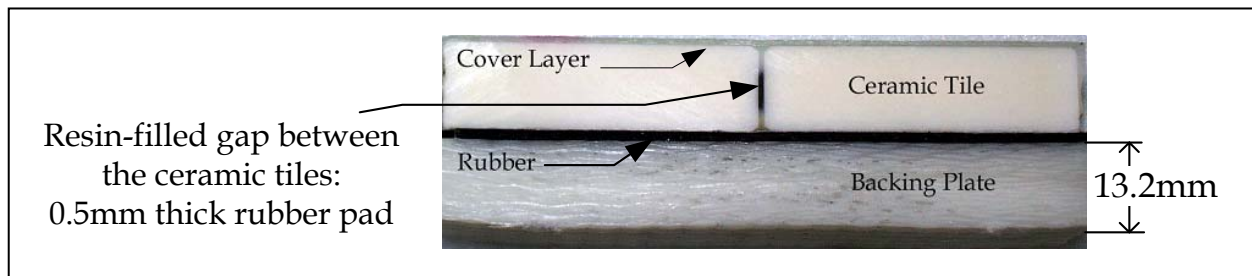


Figure 1. Cross section of a model four-layer structural armor (5).

Under ballistic impact, both the cover layer and the backing plates could be completely perforated, and the extent of damage in the ceramic tiles varied from a single tile to all of the tiles surrounding the impact site (see figure 2). Multiple interfaces in the backing plate also had delaminations that were larger than the extent of damage to the ceramic tiles (i.e., three tiles in length). Extensive fiber damage also occurred at the impact site. Experiments have shown that such damage degrades the ballistic performance of the structural armor (8). The compression strength after ballistic impact was also shown to drop to levels approaching 25% of the virgin strength (9). Repair that is capable of renewing the structural and ballistic performance after a ballistic impact is a key issue for the use of composites for Future Combat Systems (FCS).

The extent of damage in different layers determines the level of repair to be performed. Different repair strategies and repair methods that use conventional repair techniques or induction curing techniques have been documented in previous studies (8, 10). Three levels of repair have been identified according to the level of damage through the thickness of the armor. Level I is concerned with the repair of the cover layer only, as in the case of damage due to a low-velocity impact. Level II represents the case of the repair of both the cover layer and the ceramic strike face. Finally, Level III addresses the repair of all the layers that compose the

structure, including the repair of the composite backing plate, as in the case of the high-velocity ballistic impact damage shown in figure 2. A repair by resin infusion was attempted (8), but it was shown to provide only moderate improvement in the ballistic performance of the repaired panels. Because resin infusion does not effectively repair fiber damage, the present study evaluates a scarf repair that enables all damaged materials to be replaced for Level III repairs.

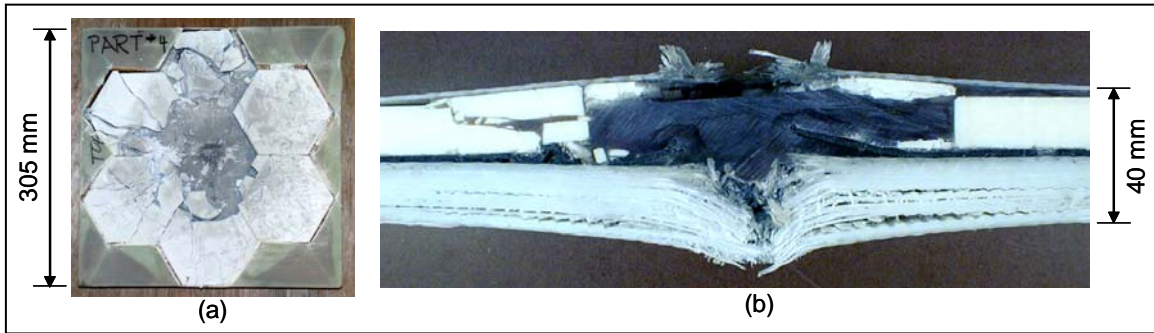


Figure 2. Ballistic damage of a composite structural armor: (a) the ceramic tiles after the cover layer have been removed and (b) cross section (8).

The repair should renew stiffness, strength, and ballistic performance to meet design requirements. The present effort on scarf repair builds on the procedures developed by Gama et al. (10) who demonstrated a Level III repair of structural armor. The repair involved the removal and replacement of all the layers shown in figure 1, including that of the composite backing plate. Following the removal of the damaged cover layer and the damaged ceramic tiles, the damaged region of the backing plate was removed using a wet grinding tool to form a circular hole. The edge of the hole was machined to produce a 45° scarf angle. The backing plate was then repaired with an adhesive-bonded flush scarf plug of the same material, and the ceramic and cover layer were replaced. The repair to the thin cover layer used a flush plug repair (i.e., butt joint). The repair of the entire cross-section was done in a single-step operation from one-side that used a vacuum bag for consolidation and induction heating for rapid heating and cure. Various susceptors were used at the various interfaces to locally heat the adhesive bond lines to cure temperatures without overheating any single interface. A repaired demonstrator panel was manufactured to prove process viability, but was not tested. These repair techniques were used in the present study to fabricate test specimens to characterize the structural performance of the backing plate with scarf repair subjected to static and dynamic loading.

Composite structural armor is subjected to bending moments and shear forces due to terrain-induced loads and lateral impacts. Some understanding of the complex interaction between layers of structural armor is needed to establish simple test methods that evaluate Level III repair approaches and maintain some relevance to the application loads. In previous work (11), the finite element method was used to model the deformation behavior of the armor in bending. The through-thickness strain distribution deviates greatly from that of the linear classical analysis due to the compliant rubber layer that decouples the ceramic from the composite backing plate. These results show that it is possible to idealize the behavior of the backing plate in the structural

armor as a beam subjected to bending loads. In addition, in-plane axial compression loads can also be used to evaluate the strength of bonded joints. The present study focused on developing simple test methods to quantify the performance of scarf-repaired thick-section composite backing plates of composite structural armor.

2. Test Methods

The four-point bending test was selected to characterize the static behavior of the virgin and repaired beams. The nominal dimension of the test beam was $889 \times 30 \times 13.2$ mm. The support span was 762 mm, which provided a span-to-thickness ratio of 57.7. The span of the loading noses was sufficiently large (381 mm) to include the scarf repair. The specimen and test configurations are shown in figure 3. An Instron 8562 (servo-hydraulic) machine equipped with a custom built four-point bend test fixture (support and loading nose diameter of 25.4 mm) was used to conduct the experiment at a constant crosshead displacement rate of 2.5 mm/min. Load and crosshead displacement data were collected using the Instron Series IX data acquisition software.

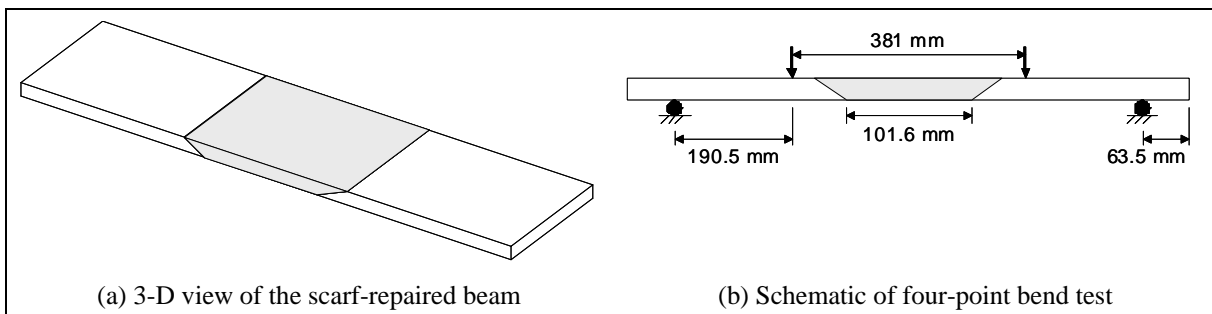


Figure 3. Four-point bending testing of scarf-repaired composite backing plate.

Dynamic axial compression tests of scarf-repaired composite joints were performed using the compression split Hopkinson pressure bar (SHPB) technique (12) (figure 4). The results generated were representative of the response of the scarf repair joints loaded in axial compression. The striker bar, the incident bar, and the transmitter bar were all made from Inconel 718 alloy (Young's modulus—200 GPa, bar velocity—4920 m/s, Poisson's ratio—0.29, and diameter—19.05 mm). Specimens of a nominal cross section (13.5×13.5 mm) were machined from scarf-repaired composite plates. The lengths of the specimens were 37.5, 70, and 90 mm for 45, 18.4, and 11.3° scarf angles, respectively. In order to load such long specimens for sufficient duration, a long striker bar (711 mm) was used to produce a long incident pulse. A rubber disk was used between the striker bar and the incident bar to shape the pulse and to uniformly load the specimen. The impact velocity of the striker bar was varied between 5 and 10 m/s, which produced a displacement rate of 2.5–5 m/s. Maximum force at failure was calculated using a “3-wave” analysis from the incident, reflected, and transmitted stress pulses as obtained from each test. A minimum of two specimens was tested for each scarf ratio and adhesive used.

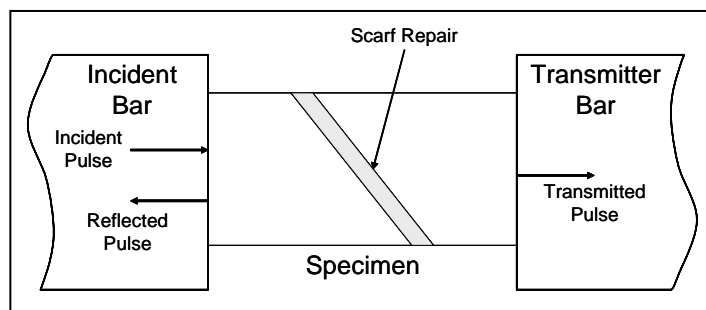


Figure 4. Hopkinson bar procedure for dynamic axial compression of scarf repair composite specimens.

3. Materials and Repair Procedure

3.1 Materials

The backing plate considered in the present work consisted of 22 layers of Knytex plain weave S-2 Glass* fabric of areal density 0.81 kg/m^2 . The lay-up orientation used was $(0^\circ/90^\circ)$ (i.e., the fabric warp direction is at 0° , and the weft direction is at 90°). The backing plates were fabricated by VARTM (5), using an Applied Poleramic SC15 epoxy resin system, specifically developed for the VARTM process. SC15 has a tensile modulus of 2.7 GPa and strain to failure of 6%. The SC15 system gels at room temperature (8–12 hr). Additionally, a 4-hr post-cure at 149°C was used. The total thickness of the backing plate was nominally 13.2 mm with a volume fraction of ~50% and <1% void content.

The choice of a proper adhesive system for repair of structures is always crucial. The selected adhesive must offer good mechanical properties, high toughness, and meet service temperature requirements. It has to be polyvalent and adhere well to different materials. Also, a moderate viscosity is needed to fill the gaps in between the ceramic tiles and the adhesive should be easily spread. Finally, cure at a relatively low temperature in a short period of time is desirable.

Four adhesives were chosen for this study that offered a broad range of properties. The Dexter Hysol† EA9359.3NA adhesive is a two-part system that cures at 82°C for 1 hr. According to the manufacturer's datasheet (13), it has a bulk tensile modulus of 2.2 GPa, a tensile strength of 31 MPa, and an elongation at failure of 10%. The Dexter Hysol EA9394 adhesive is also a two-part system that cures at 66°C for 1 hr. According to the manufacturer's datasheet (13), it has a bulk tensile modulus of 4 GPa, a tensile strength of 46 MPa, and a much lower elongation at failure of 1.7%. Both systems have been successfully cured using induction heating of structural armor. The use of a room-temperature cure adhesive was also considered. Plexus‡

* S-2 Glass is a registered trademark of Owens Corning.

† Hysol is a registered trademark of the Dexter Corporation.

‡ Plexus is a registered trademark of ITW Plexus, a business unit of Illinois Tool Works.

MA425 is a two-part methacrylate adhesive that cures in 30 min at room temperature. This adhesive provides good gap filling capability as well as a much higher elongation to failure (120%). This adhesive has a lower tensile modulus (345 MPa) and strength (17 MPa) compared to the elevated temperature cure adhesives. The fourth adhesive was also a methacrylate (Plexus AO420), which has similar mechanical properties, but a much lower curing time of 6 min.

3.2 Repair Procedure

The scarf patch repair concept shown in figure 3 is a very efficient way of repairing highly loaded composite structures. Care must normally be taken to ensure that the scarf angle is low enough to allow for a smooth stress transfer between the two adherends. Scarf repairs of thin aerospace structures are commonly limited to angles ranging between 2 and 6°. This is not practical in thick-section laminates. In the present work on the repair of thick sections, the scarf patch was limited to a diameter of 350 mm (~3 tile diameters, where extensive fiber damage occurs). Therefore, the maximum allowable scarf angle was ~11° (i.e., 1/5 scarf ratio for a 13.2-mm-thick adherend). Three scarf angles were investigated using our test methods. The angles included 45 (1/1 scarf ratio), 18.4 (1/3 scarf ratio), and 11.3° (1/5 scarf ratio).

Twenty backing plates, 889 mm long and 30 mm large, were fabricated by the VARTM process (5) and used for the characterization of the static and ballistic performance of the repairs. Two backing plates were kept virgin and tested as control beams. Eighteen beams were machined to receive the scarf patch repairs, two beams for each repair adhesive and scarf angle combination. For the repair, a distance equal to 101.6 mm separates the lower tips of the scarf, as shown in figure 3b. The placement of the repair patch only required that the surfaces in contact be completely wetted with the repair adhesive. The repair stack was then placed in a vacuum bag for hardening of the repair adhesive.

The backing plates repaired using the elevated-temperature cure Hysol adhesives were cured by induction-heating technique as described in the next section. The Plexus repaired beams were cured at room temperature. The quality of the control and repaired beams was visually observed to be very good.

4. Induction Repair

Induction heating is a noncontact method by which electrically conductive materials (susceptors) are heated in an electromagnetic field. This technique has successfully heated multiple interfaces as shown in figure 1 in a single-step operation, with the use of appropriately placed susceptors (14). A stainless steel mesh susceptor, with a wire density of $5 \times 5/\text{cm}^2$ and a wire diameter of 0.165 mm, was used in the present study. The stainless steel mesh was cut to the shape of the area to be bonded, cleaned with acetone, impregnated with adhesive, and then placed in the bond area between the parent and patch laminate (which was also covered with

adhesive). The stack was then vacuum bagged and placed horizontally under the induction coil at an optimal stand-off distance. The power setting of the induction generator, the coil shape (see figure 5), and the coil stand-off distance were selected for uniform heating of the bond line to the adhesive cure temperature. This relationship was established experimentally by using an actual repair backing plate that incorporated the susceptor mesh wrapped in a Kapton* film to allow multiple heating cycles. A two-turn rectangular coil was used for the fabrication of the 45 and 18.4° scarf repair as shown in figure 5a. A four-turn spiral coil (shown in figure 5b) was used for the fabrication of the 11.3° scarf repairs. The 11.3° scarf repairs were bonded in two passes, in order to ensure a complete coverage of the bond area with the induction-heating field. The stack was placed underneath the induction coil at a selected distance, and the power was increased from 50% to 100%, in 10% increments. Process temperatures were recorded with a thermal camera and an embedded thermocouple.

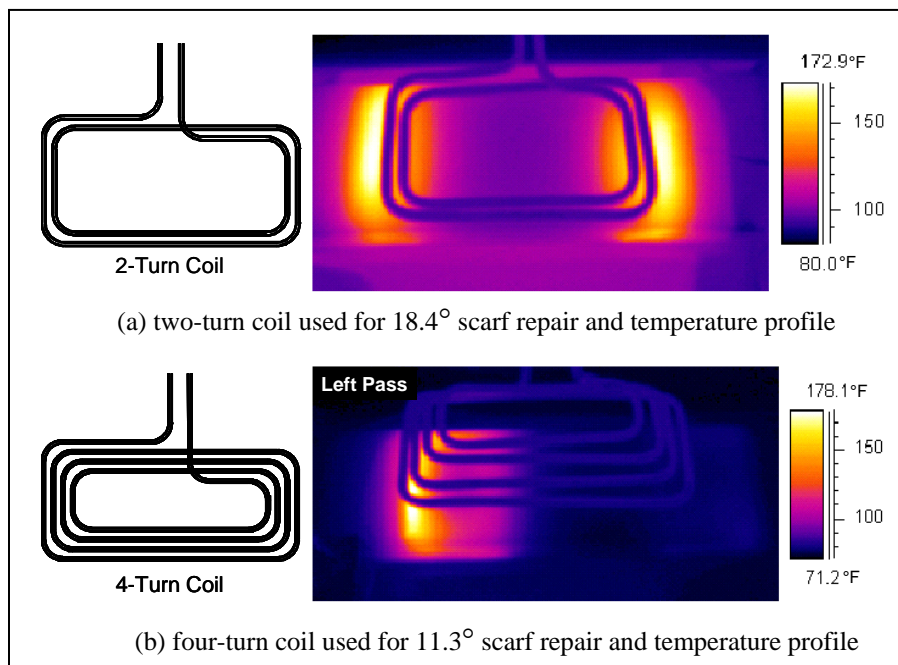


Figure 5. Induction-heating of the elevated-temperature cure adhesives.

An AGEMA Thermo-vision[†] 900 thermal camera was positioned in front of the setup to capture the full-field surface temperature of the bond area in real time. An E-type thermocouple was placed at the susceptor/adherend interface to monitor the internal bond-line temperature. The bondline temperature was slightly higher than the surface temperature due to heat losses. Steady-state was reached in a few minutes for each increment in power. Once a susceptor steady-state temperature of ~82 (i.e., the cure temperature of Hysol EA9359.3) and 66 °C (i.e., the cure temperature of Hysol EA 9394) was achievable within the range of the power

* Kapton is a registered trademark of DuPont.

[†] Thermo-vision is a registered trademark of AGEMA Company.

settings, the stand-off distance was recorded, and this combination was used for further bonding trials. The steady-state surface temperatures, recorded from the thermal camera, are presented in figure 5 for the 18.4° scarf and the 11.3° scarf repairs.

5. Static Performance of Scarf-Repaired Composite Beams

The load-deflection behavior of all the specimens tested was observed to be linear elastic until failure. Because the span-to-thickness ratio of the beams was large (i.e., 57.7), classic beam theory was used to experimentally determine the bending stiffness per unit width of the beams under four-point bending.

$$E_f I / b = (P / D_1) \cdot (L^3 / 96) / b, \quad (1)$$

where E_f is the flexural modulus, I is the moment of inertia of the cross section, P and D_1 is the instantaneous load and cross-head displacement in the linear-elastic region, L is the length of the support span, and b is the width of the beam. A comparison of the bending stiffness of the control beams with that of the repaired beams is presented in table 1. Results showed a 100% renewal of structural stiffness was attainable with the elevated-temperature cure repair adhesives. However, the room-temperature cure repaired backing plates were more compliant by ~15% due to the lower modulus of the Plexus adhesive (i.e., 0.345 vs. 2.2 GPa for EA9359.3NA). Because stiffness is typically the critical design parameter for composite armor structures, the lower stiffness of the Plexus repaired beams may prevent the use of the Plexus adhesive for repair of composite armor. However, it should be pointed out that the stiffness loss in a 3-D scarf repair is likely to be less than that measured in the 2-D beam specimen.

Table 1. Bending stiffness (per unit width) of the repaired backing plates.

Repair Type	Bending Stiffness (kN-m)
Undamaged	5.75
Elevated-temperature cure repaired	5.75
Room-temperature cure repaired	5.00

The strength renewal of repaired beams was evaluated using the ratio of moment capacity of a repaired beam to that of the control beam. The two baseline specimens (i.e., no repair) failed at an average bending moment of 8.79 kN-m/m (per unit width). The failure mode was observed to be a compressive failure of the fibers on the specimen surface layer. This failure mode did not cause catastrophic failure of the beam, and only a minor change in compliance resulted. However, the moment capacity at the onset of damage was used as the baseline for quantifying the effectiveness of the repairs. The bending moment at failure of all the repaired backing plates tested is summarized in table 2. The values given are an average value from two beams tested with minimal variation. In general, a major reduction in the moment capacity was observed and

Table 2. Bending moment at failure of the repaired baking plates.

Bending moment at failure / unit width (kN-m/m) ^a				
	Hysol EA9359.3NA	Hysol EA9394	Plexus MA425	Plexus AO420
45° scarf (1/1)	1.97	1.65	1.13	0.95
18.4° scarf (1/3)	4.60	3.34	3.36	4.05
11.3° scarf (1/5)	5.49	3.83	5.91	5.44

^aTo be compared with that of control beams, i.e., 8.79 kN-m/m.

was strongly dependent on scarf angle and adhesive type. Furthermore, the repaired beams failed suddenly at the adhesive bond line (in contrast to the progressive failure of the baseline). The extent of strength renewal (i.e., renewal of bending moment capacity), with respect to scarf angles and repair adhesives, is shown in figure 6a and 6b and ranges from 10% to 60%. The strength renewal of the induction-cured Hysol adhesives is shown in figure 6a. The repair efficiency of the 45° scarf angle was low (~20%) and was almost independent of the adhesive system used. The structural performance of the 18.4 and 11.3° scarf angles improved significantly as the scarf angle was reduced. It is observed in figure 6a that the Hysol EA9359.3 repaired beams restored as much as 62% of the control strength of the backing plates, compared with only 43% for the beams repaired with the EA9394 adhesive. The improved performance of the Hysol EA9359.3 may be attributed to the higher elongation and toughness of this adhesive system. In a recent study (15), induction-cured EA9359.3 single-lap shear joints tested in tension and four-point bending were also shown to be stronger and tougher than similar EA9394 joints.

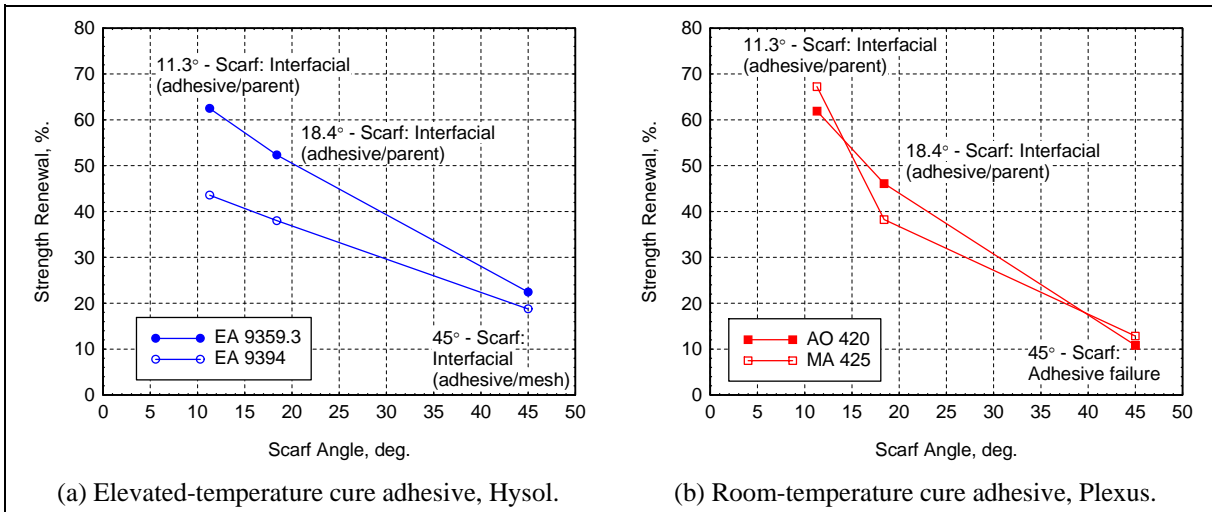


Figure 6. The renewal in static strength of the repaired backing plates.

The loci of failure of the repaired backing plates were, nevertheless, found to be similar for both elevated-temperature cure repair systems. The 45° scarf-repaired beams were seen to fail by an interfacial failure at the adhesive/metal mesh interface. Decreasing the scarf angle to 18.4°

resulted in a slight change in the failure mode, and the locus of failure was observed to be interfacial, but 50% between the metal mesh susceptor and the adhesive (top end of the scarf), and 50% between the adhesive and the parent (lower end of the scarf). The 11.3° scarf-repaired beams failed by an adhesive/parent interfacial failure. Some adherend failure was also observed to have occurred.

The strength renewal with respect to scarf angle for the Plexus adhesives is shown in figure 6b. The structural performance was mainly dependent on the scarf angle because the adhesive properties were similar. The repair efficiency was slightly lower (~10%) for the 45° scarf angle compared to the Hysol adhesives. However, the repair efficiency increased to 40% and 65% for the 18.4 and 11.3° scarf-repaired backing plates, respectively. This level was comparable to that of the induction-cured EA9359.3NA repaired backing plates. The locus of failure of the 45° scarf was in the adhesive. Decreasing the scarf angle to 18.4° promoted a mixed, adhesive/interfacial failure. The 11.3° scarf-repaired backing plates failed by interfacial failure. In summary, the 11.3° scarf angle enabled renewal of moment capacity approaching 65% of the static baseline. This range of scarf angles is considered practical for the repair of thick-section backing plates used in structural armor.

6. Dynamic Axial Compression of Scarf-Repaired Composite Plates

Dynamic axial compression of scarf-repaired composite specimens was performed using the Hopkinson bar technique. The Hopkinson bar responses for Hysol EA9359.3 adhesive repaired specimens are presented in figure 7. All of these specimens failed under dynamic loading. At lower impact velocity, a rubber pulse shaper generates an incident pulse that is almost triangular in shape. The incident pulse becomes trapezoidal in shape at higher impact velocities. The 11.3° scarf specimens did not fail when the pulse shaper was used, and thus these tests were performed without a pulse shaper.

The incident, reflected, and transmitted pulses were used to calculate the forces at the incident bar-specimen (IB-S) and specimen-transmitter bar (S-TB) interfaces, F_1 and F_2 , respectively, following the procedure described in reference (12). The condition of stress equilibrium was checked using the nonequilibrium parameter, $R = 2(F_1 - F_2) / (F_1 + F_2)$ (15). Figure 8 shows the bar-specimen interface forces and the nonequilibrium parameter calculated for the 45 and 11.3° specimens (bar responses presented in figure 7). Stress equilibrium ($R = 0.09$) was achieved in the 45° specimen only at maximum/failure load. However, better stress equilibrium was achieved in the 11.3° specimen ($R = 0.06$ at failure). The average maximum force, F_{\max} , was used to calculate the average axial strength of the specimen. Because the thickness of the adhesive bond is small as compared to the length of the incident bar, it is assumed that a volume element in the adhesive layer is under stress equilibrium (see figure 9). The axial strength was then transformed into normal and shear stresses along the failure plane (figure 9b).

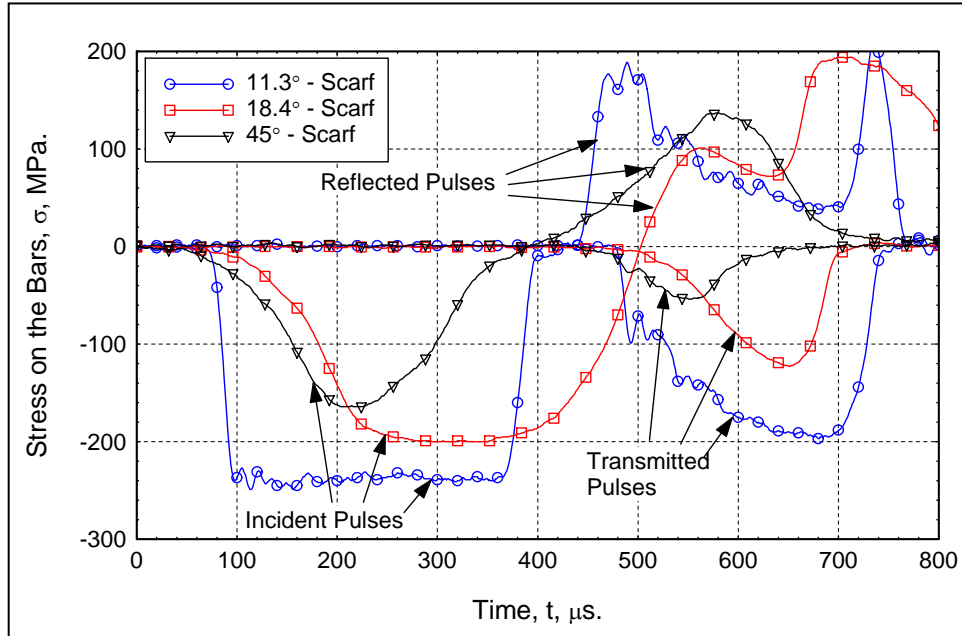


Figure 7. Hopkinson bar responses of Hysol EA9359.3 induction-cured scarf-repaired composite specimens under axial compression.

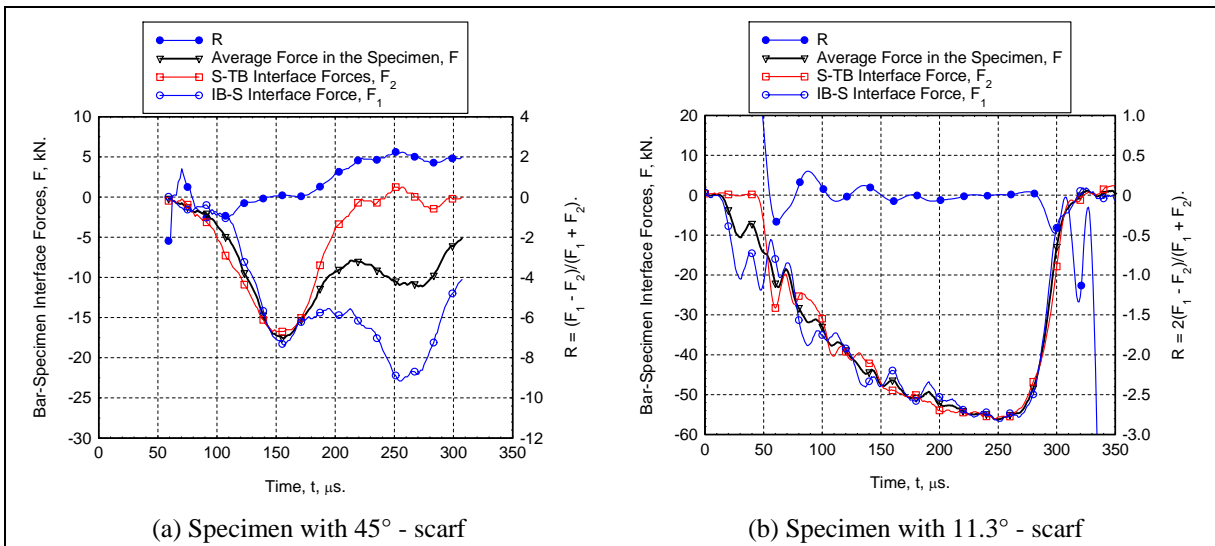


Figure 8. Stress equilibrium in Hysol EA9359.3 scarf-repaired composite specimens.

Figure 10 shows a plot of axial strength of the specimen as a function of scarf angle for quasi-static and dynamic loading cases for the various adhesives. One important observation from these tests is that the dynamic axial strengths of the scarf joints were higher than the quasi-static axial strength by a factor of 2-3 for each scarf angle. The influence of scarf angle was similar to the results shown in figure 5 for the four-point beam tests. The dynamic axial strength increased as the scarf angle decreased, for all adhesives under dynamic and quasi-static loading conditions (with the 11.3° scarf-repaired Plexus MA425 specimen being the exception).

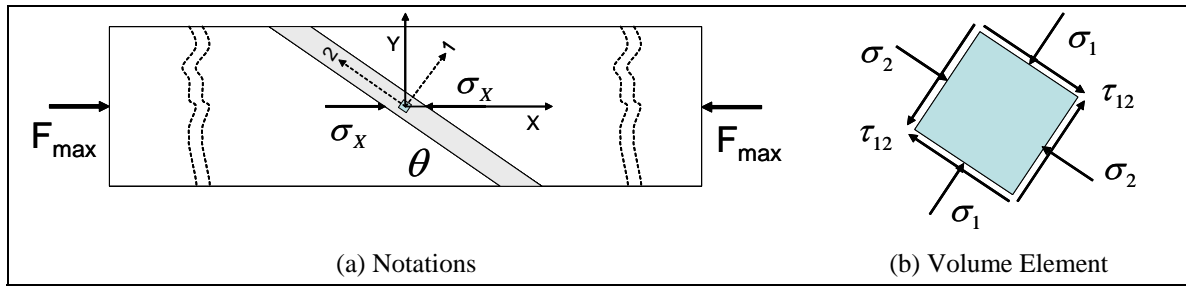


Figure 9. Stress analysis of scarf-repaired composite specimens under dynamic axial compressive load.

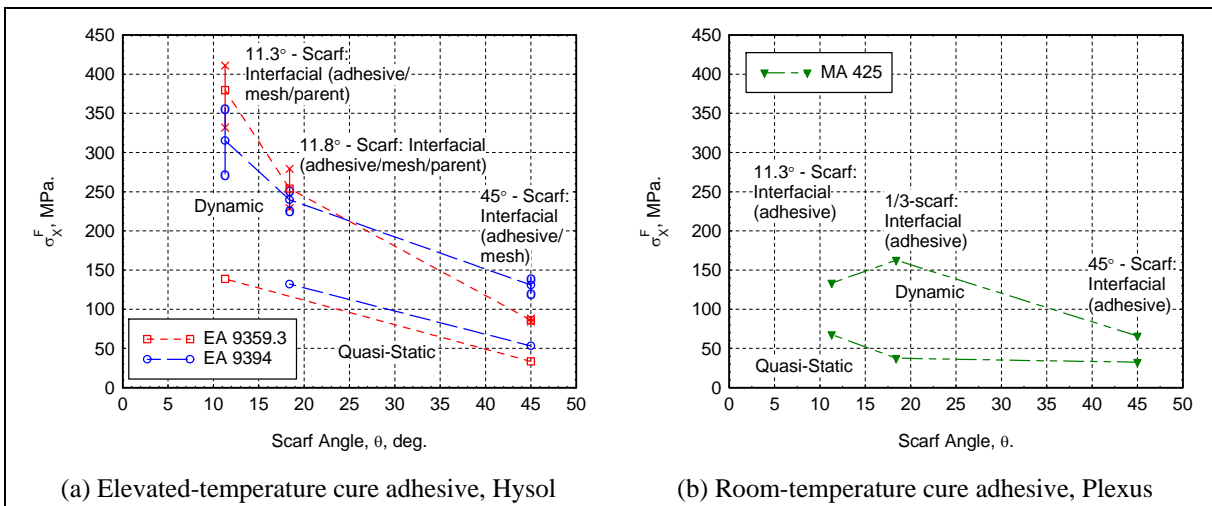


Figure 10. Axial compressive strength of scarf-repaired composite specimens under dynamic compressive load.

The loci of failure were found to be 50% in the adhesive/metal mesh interface and 50% between the adhesive and parent material in the case of Hysol adhesives (figure 11a), except for the 45° scarf for which the failure was 100% in the adhesive metal mesh interface. In the case of the Plexus adhesive joint, the loci of failure were found to be in the adhesive (figure 11b). These failure patterns were very similar to those obtained from quasi-static four-point bend tests.

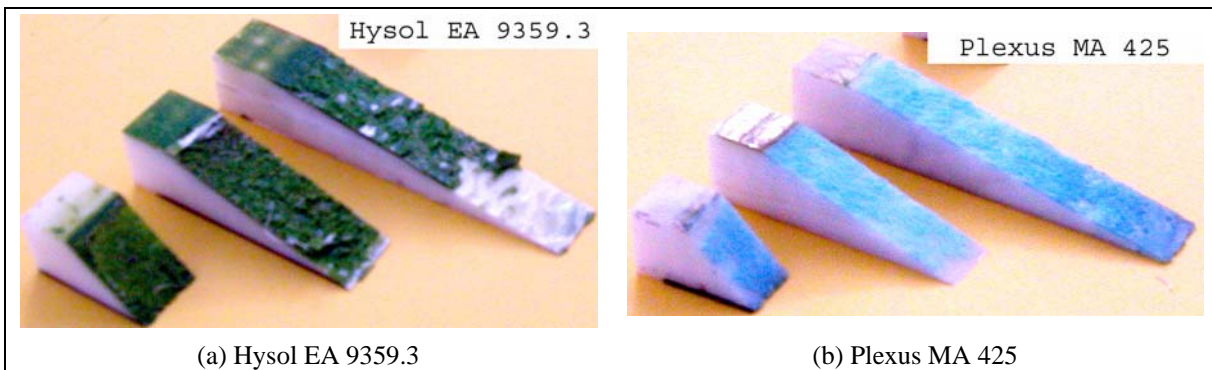


Figure 11. Fracture surfaces of scarf-repaired composite specimens under dynamic axial compression.

The axial compressive strength for the Hysol 9359.3 adhesive together with the transformed stresses in the scarf plane are presented in figure 12a. Results showed that the adhesive bond was subjected to normal compressive stress that varied significantly with the scarf angle. However, the shear stress was relatively constant in the range of 40–60 MPa. This suggested that the failure was governed by the shear stress component. In figure 12b, shear stresses of various adhesives are compared in case of static and dynamic loads. The results showed that the dynamic shear stresses at failure were significantly higher than those obtained under static loading. Furthermore, the Hysol adhesives offered higher dynamic shear strength compared to the Plexus adhesive.

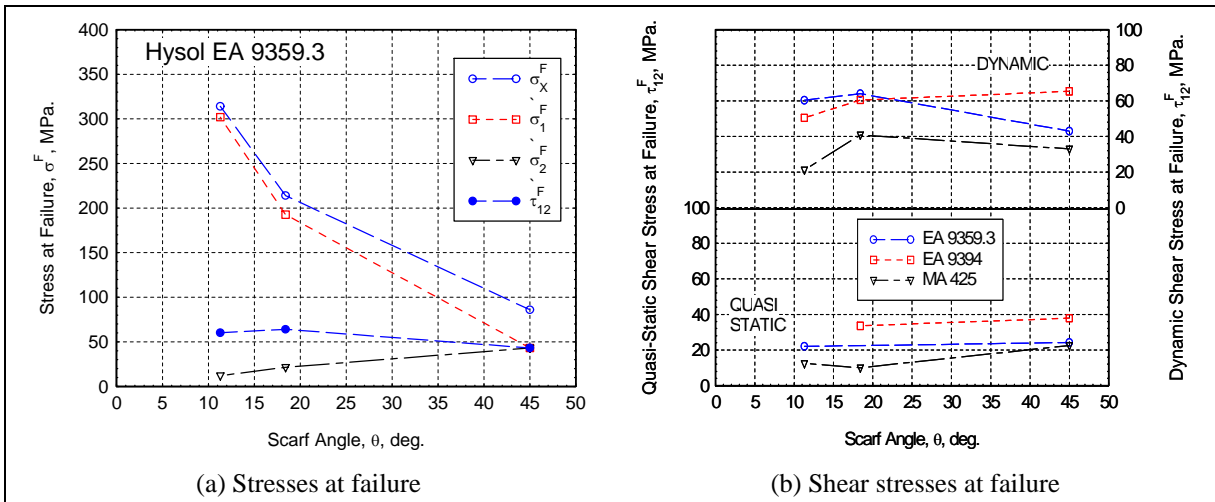


Figure 12. Stresses at failure in the rotated coordinate system of the scarf-repaired composite specimens.

7. Conclusions

The scarf patch repair scheme used in the present study is viable for level III repair of composite structural armor. The scheme uses practical scarf geometries for thick-section applications, requires only one-sided access for repair and vacuum consolidation, and provides rapid heating via induction to cure adhesives at elevated temperatures. The repair procedure was demonstrated using four adhesive systems. Simple test methods were proposed to apply realistic static and dynamic loads to composite backing plates with scarf repairs.

The repair efficiency of scarf repairs, having scarf angles much greater than commonly used in aerospace applications, was assessed in a four-point bending test. The baseline behavior exhibited compression failure on the specimen surface followed by progressive failure. Scarf-repaired beams failed catastrophically in the adhesive bond, while the virgin specimens exhibited a progressive compressive failure of the fibers on the specimen surface layer. This

difference in failure mode may indicate that the inherent energy-absorbing mechanisms of the composite were limited by the repair.

The results, however, have shown that complete renewal of stiffness is achievable for the elevated temperature cure adhesives (a slight reduction of 15% is measured for the low modulus adhesive). The degree of strength recovered (based on first damage in the baseline) from the repairs increased from ~10% to 20%, to 40%, and 60% for the 45, 18.4, and 11.3° scarf repairs, respectively.

In the dynamic experiments, scarf-repaired composite backing plates were subjected to compression loading using the SHPB. The dynamic axial strength for all adhesives was higher than the corresponding quasi-static data by a factor of 2-3 for each scarf angle. The dynamic axial strength increased as the scarf angle decreased, consistent with the four-point bend tests. The results showed that the dynamic shear strength in the scarf plane was also rate dependent and significantly greater than the static strengths. Higher rate impact testing is needed to fully characterize the strength and energy absorption capabilities of the scarf repair.

Based on the limited results generated for the adhesives considered in the present study, induction curing of Hysol EA9359.3 with a 11.3° scarf offered the best combination of structural and rate-dependent properties.

8. References

1. Gama, B. A.; Bogetti, T. A.; Fink, B. K.; Yu, C. J.; Claar, T. D.; Eifert, H. H.; Gillespie J. W., Jr. Aluminum Foam Integral Armor: A New Dimension in Armor Design. *Composite Structures* **2001**, *52*, 381–395.
2. Gama, B. A.; Gillespie, J. W., Jr.; Bogetti, T. A.; Fink, B. K. Innovative Design and Ballistic Performance of Lightweight Composite Integral Armor. *Technology for the U.S. Army's Transformation, SAE World Congress and Exposition*; paper no. 2001-01-0888; Detroit, MI, 5–8 March 2001.
3. Gama, B. A.; Gillespie, J. W., Jr. Mahfuz, H.; Bogetti, T. A.; Fink, B. K. Effect of Non-Linear Material Behavior on the Through-Thickness Stress Wave Propagation in Multi-Layer Hybrid Lightweight Armor. *International Conference on Computational Engineering and Sciences*, Los Angeles, CA, 21–25 August 2000; Atluri, S. N., Burst, F. W., Eds.; Tech Science Press: Palmdale, CA, Vol. I, pp 157–162.
4. Monib, A. M.; Gillespie, J. W., Jr. Damage Tolerance of Composite Laminates Subjected to Ballistic Impact. *Proceedings of ANTEC 98*, Society of Plastics Engineers, Brookfield, CT, 1998; pp 1463–1467.
5. Mahdi, S.; Gama, B. A.; Yarlagadda, S.; Gillespie, J. W., Jr. Effect of the Manufacturing Process on the Interfacial Properties and Structural Performance of Multi-Functional Composite Structures. *Composites Part A* **2003**, *34*, 635–647.
6. Huang, X. G.; Gillespie, J. W., Jr.; Kumar, V.; Gavin, L. Mechanics of Integral Armor: Discontinuous Ceramic-Cored Sandwich Structure Under Tension and Shear. *Composite Structures* **1996**, *36*, 81–90.
7. Davila, C. G.; Chen, T-K. Advanced Modeling Strategies for the Analysis of Tile-Reinforced Composite Armor. *Applied Composite Materials* **2000**, *7* (1), 51–68.
8. Gama, B. A.; Bogetti, T. A.; Fink, B. K.; Gillespie, J. W., Jr. Processing, Ballistic Testing and Repair of Composite Integral Armor, *Proceedings of the 32nd International SAMPE Technical Conference*, Boston, MA, 5–9 November 2000.
9. Gillespie, J. W., Jr.; Monib, A. M.; Carlsson, L. A. Damage Tolerance of Thick-Section S-2 Glass Fabric Composites Subjected to Ballistic Impact Loading. *Journal of Composite Materials* **January 2003**.

10. Gama, B. A.; Yarlagadda, S.; Bogetti, T. A.; Fink, B. K.; Gillespie, J. W., Jr. Repair of Composite Integral Armor. *Proceedings of the SAMPE 2001 Symposium and Exhibition, Materials and Processes*, Long Beach, CA, 6–10 May 2001.
11. Mahdi, S.; Gillespie, J. W., Jr. Finite Element Analysis of Tile-Reinforced Composite Structural Armor Subjected to Bending Loads. *Composites B: Engineering* **May 2003**.
12. *ASM Handbook, Volume 8, Mechanical Testing and Evaluation*; ASM International: Materials Park, OH, 2000.
13. Loctite Aerospace. Dexter Hysol Paste Adhesive and Specialty Resins Selector Guide. www.loctiteaero.com (accessed 2001).
14. Mahdi, S.; Kim, H.-J.; Gama, B. A.; Yarlagadda, S.; Gillespie, J. W., Jr. A Comparison of Oven-Cured and Induction-Cured Adhesively Bonded Composite Joints. *Journal of Composite Materials* **2003**, 37 (6), 519–542.
15. Ravichandran, G.; Subhash, G. Critical Appraisal of Limiting Strain Rates for Compression Testing of Ceramics in a Split-Hopkinson Pressure Bar. *J. Am. Ceram. Soc.* **1994**, 77, 263–267.

NO. OF
COPIES ORGANIZATION

1 DEFENSE TECHNICAL
(PDF INFORMATION CTR
ONLY) DTIC OCA
8725 JOHN J KINGMAN RD
STE 0944
FT BELVOIR VA 22060-6218

1 COMMANDING GENERAL
US ARMY MATERIEL CMD
AMCRDA TF
5001 EISENHOWER AVE
ALEXANDRIA VA 22333-0001

1 INST FOR ADVNCD TCHNLGY
THE UNIV OF TEXAS
AT AUSTIN
3925 W BRAKER LN STE 400
AUSTIN TX 78759-5316

1 US MILITARY ACADEMY
MATH SCI CTR EXCELLENCE
MADN MATH
THAYER HALL
WEST POINT NY 10996-1786

1 DIRECTOR
US ARMY RESEARCH LAB
IMNE AD IM DR
2800 POWDER MILL RD
ADELPHI MD 20783-1197

3 DIRECTOR
US ARMY RESEARCH LAB
AMSRD ARL CI OK TL
2800 POWDER MILL RD
ADELPHI MD 20783-1197

3 DIRECTOR
US ARMY RESEARCH LAB
AMSRD ARL CS IS T
2800 POWDER MILL RD
ADELPHI MD 20783-1197

NO. OF
COPIES ORGANIZATION

ABERDEEN PROVING GROUND

1 DIR USARL
AMSRD ARL CI OK TP (BLDG 4600)

NO. OF
COPIES ORGANIZATION

1 DIRECTOR
US ARMY RESEARCH LAB
AMSRD ARL SE L
D SNIDER
2800 POWDER MILL RD
ADELPHI MD 20783-1197

1 DIRECTOR
US ARMY RESEARCH LAB
AMSRD ARL SE DE
R ATKINSON
2800 POWDER MILL RD
ADELPHI MD 20783-1197

5 DIRECTOR
US ARMY RESEARCH LAB
AMSRD ARL WM MB
A ABRAHAMIAN
M BERMAN
M CHOWDHURY
T LI
E SZYMANSKI
2800 POWDER MILL RD
ADELPHI MD 20783-1197

1 COMMANDER
US ARMY MATERIEL CMD
AMXMI INT
5001 EISENHOWER AVE
ALEXANDRIA VA 22333-0001

2 PM MAS
SFAE AMO MAS MC
PICATINNY ARSENAL NJ
07806-5000

3 COMMANDER
US ARMY ARDEC
AMSTA AR CC
M PADGETT
J HEDDERICH
H OPAT
PICATINNY ARSENAL NJ
07806-5000

2 COMMANDER
US ARMY ARDEC
AMSTA AR AE WW
E BAKER
J PEARSON
PICATINNY ARSENAL NJ
07806-5000

NO. OF
COPIES ORGANIZATION

1 COMMANDER
US ARMY ARDEC
AMSTA AR FSE
PICATINNY ARSENAL NJ
07806-5000

1 COMMANDER
US ARMY ARDEC
AMSTA AR TD
PICATINNY ARSENAL NJ
07806-5000

13 COMMANDER
US ARMY ARDEC
AMSTA AR CCH A
F ALTAMURA
M NICOLICH
M PALATHINGUL
D VO
R HOWELL
A VELLA
M YOUNG
L MANOLE
S MUSALLI
R CARR
M LUCIANO
E LOGSDEN
T LOUZEIRO
PICATINNY ARSENAL NJ
07806-5000

1 COMMANDER
US ARMY ARDEC
AMSTA AR CCH P
J LUTZ
PICATINNY ARSENAL NJ
07806-5000

1 COMMANDER
US ARMY ARDEC
AMSTA AR FSF T
C LIVECCHIA
PICATINNY ARSENAL NJ
07806-5000

1 COMMANDER
US ARMY ARDEC
AMSTA ASF
PICATINNY ARSENAL NJ
07806-5000

<u>NO. OF COPIES</u>	<u>ORGANIZATION</u>
1	COMMANDER US ARMY ARDEC AMSTA AR QAC T C J PAGE PICATINNY ARSENAL NJ 07806-5000
1	COMMANDER US ARMY ARDEC AMSTA AR M D DEMELLA PICATINNY ARSENAL NJ 07806-5000
3	COMMANDER US ARMY ARDEC AMSTA AR FSA A WARNASH B MACHAK M CHIEFA PICATINNY ARSENAL NJ 07806-5000
2	COMMANDER US ARMY ARDEC AMSTA AR FSP G M SCHIKSNIS D CARLUCCI PICATINNY ARSENAL NJ 07806-5000
2	COMMANDER US ARMY ARDEC AMSTA AR CCH C H CHANIN S CHICO PICATINNY ARSENAL NJ 07806-5000
1	COMMANDER US ARMY ARDEC AMSTA AR QAC T D RIGLIOSO PICATINNY ARSENAL NJ 07806-5000
1	COMMANDER US ARMY ARDEC AMSTA AR WET T SACHAR BLDG 172 PICATINNY ARSENAL NJ 07806-5000

<u>NO. OF COPIES</u>	<u>ORGANIZATION</u>
1	US ARMY ARDEC INTELLIGENCE SPECIALIST AMSTA AR WEL F M GUERRIERE PICATINNY ARSENAL NJ 07806-5000
10	COMMANDER US ARMY ARDEC AMSTA AR CCH B P DONADIA F DONLON P VALENTI C KNUTSON G EUSTICE K HENRY J MCNABOC G WAGNECZ R SAYER F CHANG PICATINNY ARSENAL NJ 07806-5000
6	COMMANDER US ARMY ARDEC AMSTA AR CCL F PUZYCKI R MCHUGH D CONWAY E JAROSZEWSKI R SCHLENNER M CLUNE PICATINNY ARSENAL NJ 07806-5000
1	PM ARMS SFAE GCSS ARMS BLDG 171 PICATINNY ARSENAL NJ 07806-5000
1	COMMANDER US ARMY ARDEC AMSTA AR WEA J BRESCIA PICATINNY ARSENAL NJ 07806-5000
1	PM MAS SFAE AMO MAS PICATINNY ARSENAL NJ 07806-5000

NO. OF
COPIES ORGANIZATION

1 PM MAS
SFAE AMO MAS
CHIEF ENGINEER
PICATINNY ARSENAL NJ
07806-5000

1 PM MAS
SFAE AMO MAS PS
PICATINNY ARSENAL NJ
07806-5000

2 PM MAS
SFAE AMO MAS LC
PICATINNY ARSENAL NJ
07806-5000

1 COMMANDER
US ARMY ARDEC
PRODUCTION BASE
MODERN ACTY
AMSMC PBM K
PICATINNY ARSENAL NJ
07806-5000

1 COMMANDER
US ARMY TACOM
PM COMBAT SYSTEMS
SFAE GCS CS
6501 ELEVEN MILE RD
WARREN MI 48397-5000

1 COMMANDER
US ARMY TACOM
AMSTA SF
WARREN MI 48397-5000

1 DIRECTOR
AIR FORCE RESEARCH LAB
MLLMD
D MIRACLE
2230 TENTH ST
WRIGHT PATTERSON AFB OH
45433-7817

1 OFC OF NAVAL RESEARCH
J CHRISTODOULOU
ONR CODE 332
800 N QUINCY ST
ARLINGTON VA 22217-5600

1 US ARMY CERL
R LAMPO
2902 NEWMARK DR
CHAMPAIGN IL 61822

NO. OF
COPIES ORGANIZATION

1 COMMANDER
US ARMY TACOM
PM SURVIVABLE SYSTEMS
SFAE GCSS W GSI H
M RYZYI
6501 ELEVEN MILE RD
WARREN MI 48397-5000

1 COMMANDER
US ARMY TACOM
CHIEF ABRAMS TESTING
SFAE GCSS W AB QT
T KRASKIEWICZ
6501 ELEVEN MILE RD
WARREN MI 48397-5000

1 COMMANDER
WATERVLIET ARSENAL
SMCWV QAE Q
B VANINA
BLDG 44
WATERVLIET NY 12189-4050

1 TNG, DOC, & CBT DEV
ATZK TDD IRSA
A POMEY
FT KNOX KY 40121

2 HQ IOC TANK
AMMUNITION TEAM
AMSIO SMT
R CRAWFORD
W HARRIS
ROCK ISLAND IL 61299-6000

2 COMMANDER
US ARMY AMCOM
AVIATION APPLIED TECH DIR
J SCHUCK
FT EUSTIS VA 23604-5577

1 NSWC
DAHLGREN DIV CODE G06
DAHLGREN VA 22448

2 US ARMY CORPS OF ENGR
CERD C
T LIU
CEW ET
T TAN
20 MASSACHUSETTS AVE NW
WASHINGTON DC 20314

NO. OF COPIES ORGANIZATION

1 US ARMY COLD REGIONS
RSCH & ENGRNG LAB
P DUTTA
72 LYME RD
HANOVER NH 03755

14 COMMANDER
US ARMY TACOM
AMSTA TR R
R MCCLELLAND
D THOMAS
J BENNETT
D HANSEN
AMSTA JSK
S GOODMAN
J FLORENCE
K IYER
D TEMPLETON
A SCHUMACHER
AMSTA TR D
D OSTBERG
L HINOJOSA
B RAJU
AMSTA CS SF
H HUTCHINSON
F SCHWARZ
WARREN MI 48397-5000

14 BENET LABS
AMSTA AR CCB
R FISCELLA
M SOJA
E KATHE
M SCAVULO
G SPENCER
P WHEELER
S KRUPSKI
J VASILAKIS
G FRIAR
R HASENBEIN
AMSTA CCB R
S SOPOK
E HYLAND
D CRAYON
R DILLON
WATERVLIET NY 12189-4050

1 USA SBCCOM PM SOLDIER SPT
AMSSB PM RSS A
J CONNORS
KANSAS ST
NATICK MA 01760-5057

NO. OF COPIES ORGANIZATION

1 NSW
TECH LIBRARY CODE 323
17320 DAHLGREN RD
DAHLGREN VA 22448

2 USA SBCCOM
MATERIAL SCIENCE TEAM
AMSSB RSS
J HERBERT
M SENNETT
KANSAS ST
NATICK MA 01760-5057

2 OFC OF NAVAL RESEARCH
D SIEGEL CODE 351
J KELLY
800 N QUINCY ST
ARLINGTON VA 22217-5660

1 NSW
CRANE DIVISION
M JOHNSON CODE 20H4
LOUISVILLE KY 40214-5245

2 NSW
U SORATHIA
C WILLIAMS CD 6551
9500 MACARTHUR BLVD
WEST BETHESDA MD 20817

2 COMMANDER
NSWC
CARDEROCK DIVISION
R PETERSON CODE 2020
M CRITCHFIELD CODE 1730
BETHESDA MD 20084

8 DIRECTOR
US ARMY NGIC
D LEITER MS 404
M HOLTUS MS 301
M WOLFE MS 307
S MINGLEDORF MS 504
J GASTON MS 301
W GSTATTENBAUER MS 304
R WARNER MS 305
J CRIDER MS 306
2055 BOULDERS RD
CHARLOTTESVILLE VA
22911-8318

<u>NO. OF COPIES</u>	<u>ORGANIZATION</u>
1	NAVAL SEA SYSTEMS CMD D LIESE 1333 ISAAC HULL AVE SE 1100 WASHINGTON DC 20376-1100
1	EXPEDITIONARY WARFARE DIV N85 F SHOUP 2000 NAVY PENTAGON WASHINGTON DC 20350-2000
8	US ARMY SBCCOM SOLDIER SYSTEMS CENTER BALLISTICS TEAM J WARD W ZUKAS P CUNNIFF J SONG MARINE CORPS TEAM J MACKIEWICZ BUS AREA ADVOCACY TEAM W HASKELL AMSSB RCP SS W NYKVIST S BEAUDOIN KANSAS ST NATICK MA 01760-5019
7	US ARMY RESEARCH OFC A CROWSON H EVERETT J PRATER G ANDERSON D STEPP D KISEROW J CHANG PO BOX 12211 RESEARCH TRIANGLE PARK NC 27709-2211
1	AFRL MLBC 2941 P ST RM 136 WRIGHT PATTERSON AFB OH 45433-7750
1	DIRECTOR LOS ALAMOS NATL LAB F L ADDESSIO T 3 MS 5000 PO BOX 1633 LOS ALAMOS NM 87545

<u>NO. OF COPIES</u>	<u>ORGANIZATION</u>
8	NSWC J FRANCIS CODE G30 D WILSON CODE G32 R D COOPER CODE G32 J FRAYSSE CODE G33 E ROWE CODE G33 T DURAN CODE G33 L DE SIMONE CODE G33 R HUBBARD CODE G33 DAHLGREN VA 22448
1	NSWC CARDEROCK DIVISION R CRANE CODE 6553 9500 MACARTHUR BLVD WEST BETHESDA MD 20817-5700
1	AFRL MLSS R THOMSON 2179 12TH ST RM 122 WRIGHT PATTERSON AFB OH 45433-7718
2	AFRL F ABRAMS J BROWN BLDG 653 2977 P ST STE 6 WRIGHT PATTERSON AFB OH 45433-7739
5	DIRECTOR LLNL R CHRISTENSEN S DETERESA F MAGNESS M FINGER MS 313 M MURPHY L 282 PO BOX 808 LIVERMORE CA 94550
1	AFRL MLS OL L COULTER 5851 F AVE BLDG 849 RM AD1A HILL AFB UT 84056-5713
1	OSD JOINT CCD TEST FORCE OSD JCCD R WILLIAMS 3909 HALLS FERRY RD VICKSBURG MS 29180-6199

<u>NO. OF COPIES</u>	<u>ORGANIZATION</u>
3	DARPA M VANFOSSEN S WAX L CHRISTODOULOU 3701 N FAIRFAX DR ARLINGTON VA 22203-1714
2	SERDP PROGRAM OFC PM P2 C PELLERIN B SMITH 901 N STUART ST STE 303 ARLINGTON VA 22203
1	OAK RIDGE NATL LAB R M DAVIS PO BOX 2008 OAK RIDGE TN 37831-6195
1	OAK RIDGE NATL LAB C EBERLE MS 8048 PO BOX 2008 OAK RIDGE TN 37831
3	DIRECTOR SANDIA NATL LABS APPLIED MECHS DEPT MS 9042 J HANDROCK Y R KAN J LAUFFER PO BOX 969 LIVERMORE CA 94551-0969
1	OAK RIDGE NATL LAB C D WARREN MS 8039 PO BOX 2008 OAK RIDGE TN 37831
4	NIST M VANLANDINGHAM MS 8621 J CHIN MS 8621 J MARTIN MS 8621 D DUTHINH MS 8611 100 BUREAU DR GAITHERSBURG MD 20899
1	HYDROGEOLOGIC INC SERDP ESTCP SPT OFC S WALSH 1155 HERNDON PKWY STE 900 HERNDON VA 20170

<u>NO. OF COPIES</u>	<u>ORGANIZATION</u>
3	NASA LANGLEY RESEARCH CTR AMSRD ARL VS W ELBER MS 266 F BARTLETT JR MS 266 G FARLEY MS 266 HAMPTON VA 23681-0001
1	NASA LANGLEY RESEARCH CTR T GATES MS 188E HAMPTON VA 23661-3400
1	FHWA E MUNLEY 6300 GEORGETOWN PIKE MCLEAN VA 22101
1	USDOT FEDERAL RAILROAD M FATEH RDV 31 WASHINGTON DC 20590
3	CYTEC FIBERITE R DUNNE D KOHLI R MAYHEW 1300 REVOLUTION ST HAVRE DE GRACE MD 21078
1	DIRECTOR NGIC IANG TMT 2055 BOULDERS RD CHARLOTTESVILLE VA 22911-8318
1	SIOUX MFG B KRIEL PO BOX 400 FT TOTTEN ND 58335
2	3TEX CORP A BOGDANOVICH J SINGLETARY 109 MACKENAN DR CARY NC 27511
1	3M CORP J SKILDUM 3M CENTER BLDG 60 IN 01 ST PAUL MN 55144-1000

NO. OF COPIES ORGANIZATION

1 DIRECTOR
DEFENSE INTLLGNC AGENCY
TA 5
K CRELLING
WASHINGTON DC 20310

1 ADVANCED GLASS FIBER YARNS
T COLLINS
281 SPRING RUN LANE STE A
DOWNINGTON PA 19335

1 COMPOSITE MATERIALS INC
D SHORTT
19105 63 AVE NE
PO BOX 25
ARLINGTON WA 98223

1 JPS GLASS
L CARTER
PO BOX 260
SLATER RD
SLATER SC 29683

1 COMPOSITE MATERIALS INC
R HOLLAND
11 JEWEL CT
ORINDA CA 94563

1 COMPOSITE MATERIALS INC
C RILEY
14530 S ANSON AVE
SANTA FE SPRINGS CA 90670

2 SIMULA
J COLTMAN
R HUYETT
10016 S 51ST ST
PHOENIX AZ 85044

2 PROTECTION MATERIALS INC
M MILLER
F CRILLEY
14000 NW 58 CT
MIAMI LAKES FL 33014

2 FOSTER MILLER
M ROYLANCE
W ZUKAS
195 BEAR HILL RD
WALTHAM MA 02354-1196

NO. OF COPIES ORGANIZATION

1 ROM DEVELOPMENT CORP
R O MEARA
136 SWINEBURNE ROW
BRICK MARKET PLACE
NEWPORT RI 02840

2 TEXTRON SYSTEMS
T FOLTZ
M TREASURE
1449 MIDDLESEX ST
LOWELL MA 01851

1 O GARA HESS & EISENHARDT
M GILLESPIE
9113 LESAINTE DR
FAIRFIELD OH 45014

2 MILLIKEN RESEARCH CORP
H KUHN
M MACLEOD
PO BOX 1926
SPARTANBURG SC 29303

1 CONNEAUGHT INDUSTRIES INC
J SANTOS
PO BOX 1425
COVENTRY RI 02816

1 ARMTEC DEFENSE PRODUCTS
S DYER
85 901 AVE 53
PO BOX 848
COACHELLA CA 92236

1 NATL COMPOSITE CTR
T CORDELL
2000 COMPOSITE DR
KETTERING OH 45420

3 PACIFIC NORTHWEST LAB
M SMITH
G VAN ARSDALE
R SHIPPELL
PO BOX 999
RICHLAND WA 99352

1 SAIC
M PALMER
1410 SPRING HILL RD STE 400
MS SH4 5
MCLEAN VA 22102

<u>NO. OF</u> <u>COPIES</u>	<u>ORGANIZATION</u>
1	ALLIANT TECHSYSTEMS INC 4700 NATHAN LN N PLYMOUTH MN 55442-2512
1	APPLIED COMPOSITES W GRISCH 333 NORTH SIXTH ST ST CHARLES IL 60174
1	CUSTOM ANALYTICAL ENG SYS INC A ALEXANDER 13000 TENSOR LANE NE FLINTSTONE MD 21530
1	AAI CORP DR N B MCNELLIS PO BOX 126 HUNT VALLEY MD 21030-0126
1	OFC DEPUTY UNDER SEC DEFNS J THOMPSON 1745 JEFFERSON DAVIS HWY CRYSTAL SQ 4 STE 501 ARLINGTON VA 22202
3	ALLIANT TECHSYSTEMS INC J CONDON E LYNAM J GERHARD WV01 16 STATE RT 956 PO BOX 210 ROCKET CENTER WV 26726-0210
1	PROJECTILE TECHNOLOGY INC 515 GILES ST HAVRE DE GRACE MD 21078
1	HEXCEL INC R BOE PO BOX 18748 SALT LAKE CITY UT 84118
1	PRATT & WHITNEY C WATSON 400 MAIN ST MS 114 37 EAST HARTFORD CT 06108

<u>NO. OF</u> <u>COPIES</u>	<u>ORGANIZATION</u>
5	NORTHROP GRUMMAN B IRWIN K EVANS D EWART A SHREKENHAMER J MCGLYNN BLDG 160 DEPT 3700 1100 WEST HOLLYVALE ST AZUSA CA 91701
1	HERCULES INC HERCULES PLAZA WILMINGTON DE 19894
1	BRIGS COMPANY J BACKOFEN 2668 PETERBOROUGH ST HERNDON VA 22071-2443
1	ZERNOW TECHNICAL SERVICES L ZERNOW 425 W BONITA AVE STE 208 SAN DIMAS CA 91773
1	GENERAL DYNAMICS OTS L WHITMORE 10101 NINTH ST NORTH ST PETERSBURG FL 33702
2	GENERAL DYNAMICS OTS FLINCHBAUGH DIV K LINDE T LYNCH PO BOX 127 RED LION PA 17356
1	GKN WESTLAND AEROSPACE D OLDS 450 MURDOCK AVE MERIDEN CT 06450-8324
2	BOEING ROTORCRAFT P MINGURT P HANDEL 800 B PUTNAM BLVD WALLINGFORD PA 19086

NO. OF
COPIES ORGANIZATION

5 SIKORSKY AIRCRAFT
G JACARUSO
T CARSTENSAN
B KAY
S GARBO MS S330A
J ADELMANN
6900 MAIN ST
PO BOX 9729
STRATFORD CT 06497-9729

1 AEROSPACE CORP
G HAWKINS M4 945
2350 E EL SEGUNDO BLVD
EL SEGUNDO CA 90245

2 CYTEC FIBERITE
M LIN
W WEB
1440 N KRAEMER BLVD
ANAHEIM CA 92806

2 UDLP
G THOMAS
M MACLEAN
PO BOX 58123
SANTA CLARA CA 95052

1 UDLP WARREN OFC
A LEE
31201 CHICAGO RD SOUTH
SUITE B102
WARREN MI 48093

2 UDLP
R BRYNSVOLD
P JANKE MS 170
4800 EAST RIVER RD
MINNEAPOLIS MN 55421-1498

1 LOCKHEED MARTIN
SKUNK WORKS
D FORTNEY
1011 LOCKHEED WAY
PALMDALE CA 93599-2502

1 LOCKHEED MARTIN
R FIELDS
5537 PGA BLVD
SUITE 4516
ORLANDO FL 32839

NO. OF
COPIES ORGANIZATION

1 NORTHRUP GRUMMAN CORP
ELECTRONIC SENSORS
& SYSTEMS DIV
E SCHOCH MS V 16
1745A W NURSERY RD
LINTHICUM MD 21090

1 GDLS DIVISION
D BARTLE
PO BOX 1901
WARREN MI 48090

2 GDLS
D REES
M PASIK
PO BOX 2074
WARREN MI 48090-2074

1 GDLS
MUSKEGON OPER
M SOIMAR
76 GETTY ST
MUSKEGON MI 49442

1 GENERAL DYNAMICS
AMPHIBIOUS SYS
SURVIVABILITY LEAD
G WALKER
991 ANNAPOLIS WAY
WOODBIDGE VA 22191

6 INST FOR ADVANCED
TECH
H FAIR
I MCNAB
P SULLIVAN
S BLESS
W REINECKE
C PERSAD
3925 W BRAKER LN STE 400
AUSTIN TX 78759-5316

1 ARROW TECH ASSOC
1233 SHELBURNE RD STE D8
SOUTH BURLINGTON VT
05403-7700

1 R EICHELBERGER
CONSULTANT
409 W CATHERINE ST
BEL AIR MD 21014-3613

<u>NO. OF COPIES</u>	<u>ORGANIZATION</u>
1	SAIC G CHRYSSOMALLIS 8500 NORMANDALE LAKE BLVD SUITE 1610 BLOOMINGTON MN 55437-3828
1	UCLA MANE DEPT ENGR IV H T HAHN LOS ANGELES CA 90024-1597
2	UNIV OF DAYTON RESEARCH INST R Y KIM A K ROY 300 COLLEGE PARK AVE DAYTON OH 45469-0168
1	UMASS LOWELL PLASTICS DEPT N SCHOTT 1 UNIVERSITY AVE LOWELL MA 01854
1	IIT RESEARCH CTR D ROSE 201 MILL ST ROME NY 13440-6916
1	GA TECH RESEARCH INST GA INST OF TCHNLGY P FRIEDERICH ATLANTA GA 30392
1	MICHIGAN ST UNIV MSM DEPT R AVERILL 3515 EB EAST LANSING MI 48824-1226
1	UNIV OF WYOMING D ADAMS PO BOX 3295 LARAMIE WY 82071
1	PENN STATE UNIV R S ENGEL 245 HAMMOND BLDG UNIVERSITY PARK PA 16801

<u>NO. OF COPIES</u>	<u>ORGANIZATION</u>
2	PENN STATE UNIV R MCNITT C BAKIS 212 EARTH ENGR SCIENCES BLDG UNIVERSITY PARK PA 16802
1	PURDUE UNIV SCHOOL OF AERO & ASTRO C T SUN W LAFAYETTE IN 47907-1282
1	STANFORD UNIV DEPT OF AERONAUTICS & AEROBALLISTICS S TSAI DURANT BLDG STANFORD CA 94305
1	UNIV OF MAINE ADV STR & COMP LAB R LOPEZ ANIDO 5793 AEWB BLDG ORONO ME 04469-5793
1	JOHNS HOPKINS UNIV APPLIED PHYSICS LAB P WIENHOLD 11100 JOHNS HOPKINS RD LAUREL MD 20723-6099
1	UNIV OF DAYTON J M WHITNEY COLLEGE PARK AVE DAYTON OH 45469-0240
1	NORTH CAROLINA ST UNIV CIVIL ENGINEERING DEPT W RASDORF PO BOX 7908 RALEIGH NC 27696-7908
5	UNIV OF DELAWARE CTR FOR COMPOSITE MTRLS J GILLESPIE M SANTARE S YARLAGADDA S ADVANI D HEIDER 201 SPENCER LAB NEWARK DE 19716

<u>NO. OF COPIES</u>	<u>ORGANIZATION</u>	<u>NO. OF COPIES</u>	<u>ORGANIZATION</u>
1	DEPT OF MTRLS SCIENCE & ENGRG UNIV OF ILLINOIS AT URBANA CHAMPAIGN J ECONOMY 1304 WEST GREEN ST 115B URBANA IL 61801		<u>ABERDEEN PROVING GROUND</u>
1	UNIV OF MARYLAND DEPT OF AEROSPACE ENGRG A J VIZZINI COLLEGE PARK MD 20742	1	US ARMY ATC CSTE DTC AT AC I W C FRAZER 400 COLLERAN RD APG MD 21005-5059
1	DREXEL UNIV A S D WANG 3141 CHESTNUT ST PHILADELPHIA PA 19104	91	DIR USARL AMSRD ARL CI AMSRD ARL O AP EG M ADAMSON AMSRD ARL SL BA AMSRD ARL SL BB D BELY AMSRD ARL WM J SMITH H WALLACE AMSRD ARL WM B A HORST T KOGLER AMSRD ARL WM BA D LYON AMSRD ARL WM BC J NEWILL P PLOSTINS A ZIELINSKI AMSRD ARL WM BD P CONROY B FORCH M LEADORE C LEVERITT R LIEB R PESCE RODRIGUEZ B RICE AMSRD ARL WM BF S WILKERSON AMSRD ARL WM M B FINK J MCCAULEY AMSRD ARL WM MA L GHIORSE S MCKNIGHT E WETZEL AMSRD ARL WM MB J BENDER T BOGETTI L BURTON R CARTER K CHO W DE ROSSET G DEWING R DOWDING W DRYSDALE
3	UNIV OF TEXAS AT AUSTIN CTR FOR ELECTROMECHANICS J PRICE A WALLS J KITZMILLER 10100 BURNET RD AUSTIN TX 78758-4497		
3	VA POLYTECHNICAL INST & STATE UNIV DEPT OF ESM M W HYER K REIFSNIDER R JONES BLACKSBURG VA 24061-0219		
1	SOUTHWEST RESEARCH INST ENGR & MATL SCIENCES DIV J RIEGEL 6220 CULEBRA RD PO DRAWER 28510 SAN ANTONIO TX 78228-0510		
1	BATELLE NATICK OPERS B HALPIN 313 SPEEN ST NATICK MA 01760		
3	DIRECTOR US ARMY RESEARCH LAB AMSRD ARL WM MB A FRYDMAN 2800 POWDER MILL RD ADELPHI MD 20783-1197		

NO. OF
COPIES ORGANIZATION

R EMERSON
D HENRY
D HOPKINS
R KASTE
L KECSKES
M MINNICINO
B POWERS
D SNOHA
J SOUTH
M STAKER
J SWAB
J TZENG
AMSRD ARL WM MC
J BEATTY
R BOSSOLI
E CHIN
S CORNELISON
D GRANVILLE
B HART
J LASALVIA
J MONTGOMERY
F PIERCE
E RIGAS
W SPURGEON
AMSRD ARL WM MD
B CHEESEMAN
P DEHMER
R DOOLEY
G GAZONAS
S GHORSE
C HOPPEL
M KLUSEWITZ
W ROY
J SANDS
D SPAGNUOLO
S WALSH
S WOLF
AMSRD ARL WM RP
J BORNSTEIN
C SHOEMAKER
AMSRD ARL WM T
B BURNS
AMSRD ARL WM TA
W BRUCHEY
M BURKINS
W GILLICH
B GOOCH
T HAVEL
E HORWATH
M NORMANDIA
J RUNYEON
M ZOLTOSKI

NO. OF
COPIES ORGANIZATION

AMSRD ARL WM TB
P BAKER
AMSRD ARL WM TC
R COATES
AMSRD ARL WM TD
D DANDEKAR
T HADUCH
T MOYNIHAN
M RAFTENBERG
S SCHOENFELD
T WEERASOORIYA
AMSRD ARL WM TE
A NILER
J POWELL

NO. OF
COPIES ORGANIZATION

1 LTD
R MARTIN
MERL
TAMWORTH RD
HERTFORD SG13 7DG
UK

1 SMC SCOTLAND
P W LAY
DERA ROSYTH
ROSYTH ROYAL DOCKYARD
DUNFERMLINE FIFE KY 11 2XR
UK

1 CIVIL AVIATION
ADMINSTRATION
T GOTTESMAN
PO BOX 8
BEN GURION INTRNL AIRPORT
LOD 70150
ISRAEL

1 AEROSPATIALE
S ANDRE
A BTE CC RTE MD132
316 ROUTE DE BAYONNE
TOULOUSE 31060
FRANCE

1 DRA FORT HALSTEAD
P N JONES
SEVEN OAKS KENT TN 147BP
UK

1 SWISS FEDERAL ARMAMENTS
WKS
W LANZ
ALLMENDSTRASSE 86
3602 THUN
SWITZERLAND

1 DYNAMEC RESEARCH LAB
AKE PERSSON
BOX 201
SE 151 23 SODERTALJE
SWEDEN

NO. OF
COPIES ORGANIZATION

1 ISRAEL INST OF TECHLGY
S BODNER
FACULTY OF MECHANICAL
ENGR
HAIFA 3200
ISRAEL

1 DSTO
WEAPONS SYSTEMS DIVISION
N BURMAN RLLWS
SALISBURY
SOUTH AUSTRALIA 5108
AUSTRALIA

1 DEF RES ESTABLISHMENT
VALCARTIER
A DUPUIS
2459 BLVD PIE XI NORTH
VALCARTIER QUEBEC
CANADA
PO BOX 8800 COURCELETTE
GOA IRO QUEBEC
CANADA

1 ECOLE POLYTECH
J MANSON
DMX LTC
CH 1015 LAUSANNE
SWITZERLAND

1 TNO DEFENSE RESEARCH
R IJSSELSTEIN
ACCOUNT DIRECTOR
R&D ARMEE
PO BOX 6006
2600 JA DELFT
THE NETHERLANDS

2 FOA NATL DEFENSE RESEARCH
ESTAB
DIR DEPT OF WEAPONS &
PROTECTION
B JANZON
R HOLMLIN
S 172 90 STOCKHOLM
SWEDEN

NO. OF
COPIES ORGANIZATION

- 2 DEFENSE TECH & PROC
AGENCY GROUND
I CREWTHER
GENERAL HERZOG HAUS
3602 THUN
SWITZERLAND

- 1 MINISTRY OF DEFENCE
RAFAEL
ARMAMENT DEVELOPMENT
AUTH
M MAYSELESS
PO BOX 2250
HAIFA 31021
ISRAEL

- 1 TNO DEFENSE RESEARCH
I H PASMAN
POSTBUS 6006
2600 JA DELFT
THE NETHERLANDS

- 1 B HIRSCH
TACHKEMONY ST 6
NETAMUA 42611
ISRAEL

- 1 DEUTSCHE AEROSPACE AG
DYNAMICS SYSTEMS
M HELD
PO BOX 1340
D 86523 SCHROBENHAUSEN
GERMANY